

UKAEA-CCFE-PR(18)41

K Imada, H R Wilson, J W Connor, A Dudkovskaia and P Hill

# **Nonlinear, kinetic ion response to small scale magnetic islands in tokamak plasmas - Neoclassical Tearing Mode Threshold Physics**

Enquiries about copyright and reproduction should in the first instance be addressed to the UKAEA Publications Officer, Culham Science Centre, Building K1/0/83 Abingdon, Oxfordshire, OX14 3DB, UK. The United Kingdom Atomic Energy Authority is the copyright holder.

# **Nonlinear, kinetic ion response to small scale magnetic islands in tokamak plasmas - Neoclassical Tearing Mode Threshold Physics**

K Imada,<sup>1</sup> H R Wilson,<sup>1,2</sup> J W Connor,<sup>2</sup> A Dudkovskaia<sup>1</sup> and P Hill<sup>1</sup>

*<sup>1</sup>York Plasma Institute, Department of Physics, University of York, Heslington, York, YO10 5DD, United Kingdom*

*<sup>2</sup>CCFE, Culham Science Centre, Abingdon, Oxon, OX14 3DB, United Kingdom*



# Nonlinear, Kinetic Ion Response to Small Scale Magnetic Islands in Tokamak Plasmas — Neoclassical Tearing Mode Threshold Physics

K Imada,<sup>1</sup> H R Wilson,<sup>1,2</sup> J W Connor,<sup>2</sup> A Dudkovskaia,<sup>1</sup> and P Hill<sup>1</sup>

<sup>1</sup>*York Plasma Institute, Department of Physics, University of York, Heslington, York, YO10 5DD, United Kingdom*

<sup>2</sup>*CCFE, Culham Science Centre, Abingdon, Oxon, OX14 3DB, United Kingdom*

(Dated: May 9, 2018)

A new drift-kinetic theory of the ion response to magnetic islands in tokamak plasmas is presented. Small islands are considered, with widths  $w$  much smaller than the plasma radius  $r$ , but comparable to the trapped ion orbit width  $\rho_{bi}$ . An expansion in  $w/r$  reduces the system dimensions from five down to four. In the absence of an electrostatic potential, the ions follow stream lines that map out a ‘drift-island’ structure that is identical to the magnetic island, but shifted by an amount  $\sim$  few  $\rho_{bi}$ . The result qualitatively holds even with the inclusion of the electrostatic potential required for quasi-neutrality. The ion distribution function is flattened across these drift islands, not the magnetic island. For large islands,  $w \gg \rho_{bi}$ , the effect of the shift is negligible. For small islands,  $w \sim \rho_{bi}$ , the shift results in a pressure gradient being maintained across the magnetic island. This suppresses the bootstrap current drive for small islands, which is an important new effect, influencing the threshold for neoclassical tearing mode instabilities — a key result for the performance of future tokamaks, including ITER.

Magnetised plasmas are susceptible to tearing mode instabilities, characterised by the evolution of magnetic islands. These arise from a filamentation of the component of current density along magnetic field lines which, in turn, creates the island structures. The change in magnetic topology associated with these islands has an impact on the confinement of the plasma by the magnetic field. It is therefore important to determine the conditions under which they grow to large amplitude. To address this, it is necessary to understand how the ions and electrons respond to magnetic islands, what currents that response creates, and whether those currents act to amplify or heal the island.

In the simplest picture, ions and electrons free-stream along magnetic field lines. As a result, their distribution functions are constant on the perturbed magnetic flux surfaces of the island. In the absence of heat and/or particle sources, this results in a flattening of the distribution function across the island O-point. In this Letter, we show that the particle drifts have a significant impact on this picture, especially when the width of particle orbits associated with those drifts are comparable to the island width. As a particular example we focus on the tokamak, which provides a good illustration of the effect because: (a) it has  $\mathbf{E} \times \mathbf{B}$ , grad-B and curvature drifts; and (b) the results have consequences for an important tokamak instability called the neoclassical tearing mode.

In tokamak plasmas, the current density filamentation that drives neoclassical tearing modes is typically dominated by the bootstrap current. In toroidal geometry, a fraction of particles are trapped in the low magnetic field region of the tokamak plasma executing closed, banana-shaped orbits. With the presence of a pressure gradient, the finite banana width of those trapped particle orbits drives opposing flows in the ions and electrons along magnetic field lines in a similar mechanism to that respon-

sible for diamagnetic flows. This seeds the aforementioned bootstrap current, that is carried by the passing (i.e. non-trapped) particles [1]. With a magnetic island present, the flattening of the pressure gradient creates a hole in the bootstrap current, and (for typical tokamak conditions) the resulting filamentation of current density leads to an amplification of the magnetic island. This is the neoclassical tearing mode (NTM) instability [2–9]. It is a major concern for ITER because, if not controlled, it causes significant confinement degradation and can even terminate the plasma discharge in a disruption.

Neoclassical theory is well-developed to describe the physics of the trapped and passing particles when their trapped banana orbit widths,  $\rho_{bi}$  and  $\rho_{be}$ , are much smaller than the length scales associated with the plasma profiles (e.g. pressure gradient). Accounting for the island geometry, the theory provides a good description of the bootstrap current drive when the islands are much wider than the ion banana width. The NTM theory then predicts that all ‘seed’ magnetic islands, however small, will grow to large amplitude with a dramatic deleterious impact on confinement. However, experiments indicate that additional mechanisms are present suppressing magnetic islands that have a half width  $w$  comparable to the trapped ion banana orbit width:  $w \sim \rho_{bi}$  [10]. This is precisely the regime where the conventional theory breaks down. To develop a quantitative understanding of this threshold phenomenon, it is necessary to extend the theory to understand: (1) how the ions respond to small islands; (2) the consequences for the perturbed bootstrap current in a tokamak; and (3) the consequences for the NTM drive. We address each of these in this Letter.

Our starting point is the drift kinetic model to describe the ion distribution function in a magnetised plasma, with electrostatic potential  $\Phi$ . Assuming that the effect of the island on plasma parameters is localised to

its vicinity, we work in the island rest frame and seek a steady state solution, neglecting any temporal fluctuation in fields (see [11] for impact of turbulence). The drift kinetic equation for the ion distribution function  $f_i$  can then be written in the time-independent form:

$$v_{\parallel} \nabla_{\parallel} f_i + \mathbf{v}_E \cdot \nabla f_i + \mathbf{v}_b \cdot \nabla f_i - \frac{Ze}{m_i} \left( \frac{v_{\parallel} \nabla_{\parallel} \Phi}{v} + \frac{\mathbf{v}_b \cdot \nabla \Phi}{v} \right) \frac{\partial f_i}{\partial v} = C_i(f_i), \quad (1)$$

where  $v$  is the particle speed ( $\parallel$  denoting a component parallel to the magnetic field,  $\mathbf{B}$ ),  $\nabla_{\parallel} = \mathbf{b} \cdot \nabla$ ,  $\mathbf{b} = \mathbf{B}/B$  and  $\mathbf{v}_E = (\mathbf{B} \times \nabla \Phi)/B^2$ .  $\mathbf{v}_b = -v_{\parallel} \mathbf{b} \times \nabla(v_{\parallel}/\omega_{ci})$  is the combination of grad- $B$  and curvature drifts,  $\omega_{ci} = ZeB/m_i$  is the ion gyrofrequency, and  $Ze$  and  $m_i$  are the ion charge and mass respectively. On the right hand side of Eq. (1) is the collision operator. Spatial derivatives are taken at constant kinetic energy  $\mathcal{E} = m_i v^2/2$  and magnetic moment  $\mu = m_i v_{\perp}^2/2$ , where  $v_{\perp}^2 = v^2 - v_{\parallel}^2$ . We define the pitch angle,  $\lambda = \mu/\mathcal{E}$ , so that  $v_{\parallel} = \sigma v \sqrt{1 - \lambda B}$  with  $\sigma = v_{\parallel}/|v_{\parallel}| = \pm 1$ .

Our choice for the radial coordinate is  $x = (\psi - \psi_s)/\psi_s$ , where  $\psi$  is the poloidal flux and  $\psi_s$  labels the rational surface where the safety factor,  $q(\psi = \psi_s) = m/n$ , with  $m$  and  $n$  being the poloidal and toroidal mode numbers of the magnetic island respectively. Our other two spatial coordinates are the straight field line poloidal angle  $\theta$  measuring the distance along an equilibrium magnetic field line, and helical angle  $\xi$  labelling the field lines at the rational surface. For a toroidally symmetric tokamak plasma, the canonical angular momentum,  $p_{\phi} = (\psi - \psi_s) - I v_{\parallel}/\omega_{ci}$ , is conserved during particle motion, where  $I(\psi) = RB_{\phi}$  with  $R$  the major radius and  $B_{\phi}$  the toroidal component of the magnetic field. Exploiting this variable is key to reducing the dimensionality of the system. We solve Eq. (1) by writing the ion distribution thus:  $f_i = (1 - Ze\Phi/T_i(0)) F_{Mi}(0) + p_{\phi} F'_{Mi}(0) + g_i$ , where (0) indicates the quantity evaluated at the rational surface, the prime denotes a differential with respect to  $\psi$ ,  $T_i$  is the ion temperature and  $F_{Mi}(0) = n_i(0) [\pi v_{thi}^2(0)]^{-3/2} \exp[-v^2/v_{thi}^2(0)]$  is the Maxwellian. Here,  $v_{thi} = \sqrt{2k_B T_i/m_i}$  is the ion thermal speed,  $n_i$  is the ion density and  $k_B$  is Boltzmann's constant.

The magnetic field of a tokamak has a maximum,  $B_{\max}$ , on the inboard side. If  $\lambda < \lambda_c \equiv B_{\max}^{-1}$ , the particles pass around the full extent of the flux surface, most of them deviating from it by a small amount  $\sim \epsilon \rho_{\theta i}$ , where  $\rho_{\theta i} = m_i v_{thi}/ZeB_{\theta}$  is the poloidal ion Larmor radius, and  $\epsilon = r/R$  is the inverse aspect ratio. If  $\lambda > \lambda_c$  the particles are trapped to the region of weaker magnetic field, bouncing between the two points  $\theta_{b\pm}$  along the field lines, where  $\lambda B(\theta = \theta_{b\pm}) = 1$ , and deviating from the flux surface by a larger amount called the ion banana width,  $\rho_{bi} \sim \epsilon^{1/2} \rho_{\theta i}$ . In a tokamak, the system size is typically much greater than  $\rho_{\theta i}$ , so we can introduce a small parameter,  $\Delta = \rho_{\theta i}/r_s$ , where  $r_s$  is the

minor radius of the rational surface where  $\psi = \psi_s$ . We wish to consider the ion response to small islands with a width  $w$  comparable to the ion banana width. Then, we seek solutions to Eq. (1) by expanding in powers of  $\Delta$ :  $g_i = \sum_k \Delta^k g_i^{(k)}$ .

Ordering  $w/r$ ,  $Ze\Phi/T_i$  and  $g_i^{(0)}/F_{Mi}(0)$  all like  $\Delta$ , the leading order contributions to Eq. (1) come from the free streaming along the magnetic field lines, as well as the radial components of the grad- $B$  and curvature drifts, which combine to give:

$$\frac{v_{\parallel}}{B} \frac{I}{R^2 q} \frac{\partial g_i^{(0)}}{\partial \theta} \Bigg|_{p_{\phi}, \xi, \lambda, v} = 0, \quad (2)$$

assuming that the collisional term on the right hand side of Eq. (1) is order  $\Delta$  smaller than this free-streaming term. We can integrate Eq. (2) to find that  $g_i$  is independent of  $\theta$  at fixed  $p_{\phi}$ , i.e.  $g_i^{(0)}(x, \theta, \xi, \lambda, v; \sigma) = \bar{g}_i^{(0)}(p_{\phi}, \xi, \lambda, v; \sigma)$ . This reduces the dimension of the problem from 5D to 4D, but the form of  $\bar{g}_i^{(0)}$  is still to be determined.

At next order we derive an equation for  $g_i^{(1)}$  in terms of  $\bar{g}_i^{(0)}$ , where the term in  $g_i^{(1)}$  has the same form as that in Eq. (2). This term is eliminated by taking the average over  $\theta$  at fixed  $p_{\phi}$ ,  $\xi$ ,  $\lambda$  and  $v$ ; equivalent to averaging over the particle orbits. For  $\lambda < \lambda_c$ , we can integrate over a period in  $\theta$ , imposing a periodic boundary condition to eliminate the term in  $g_i^{(1)}$ . In the trapped region ( $\lambda > \lambda_c$ ), we integrate between the bounce points  $\theta_{b\pm}$  and sum over the two streams,  $\sigma = \pm 1$ , which then annihilates the term in  $g_i^{(1)}$  due to continuity at each of the bounce points. Considering a large aspect ratio circular cross section tokamak, dropping terms of  $O(\epsilon^2)$  and smaller, and writing the magnetic field perturbation  $\mathbf{B}_1 = \nabla \times (A_{\parallel} \mathbf{b})$ , with  $RA_{\parallel} = -w^2 q'/(4q) f(\xi)$  ( $q' = dq/d\psi$ ) we arrive at our final equation for  $\bar{g}_i^{(0)}$ :

$$\left[ \hat{p}_{\phi} \Theta(\lambda_c - \lambda) + \omega_D - \omega_{E, \xi} \right] \frac{\partial \bar{g}_i^{(0)}}{\partial \xi} \Bigg|_{p_{\phi}} - \left[ \frac{\hat{w}^2}{4} \frac{df}{d\xi} \Theta(\lambda_c - \lambda) - \omega_{E, x} \right] \frac{\partial \bar{g}_i^{(0)}}{\partial \hat{p}_{\phi}} \Bigg|_{\xi} = \frac{\epsilon^{3/2} L_q}{q} \left\langle \frac{\nu_{*i} C_{ii}(\bar{g}_i^{(0)})}{\hat{v}_{\parallel} \nu_i} \right\rangle, \quad (3)$$

where  $\langle \dots \rangle_{\theta}$  denotes the orbit average described above. We have defined dimensionless variables  $\hat{p}_{\phi} = p_{\phi}/\psi_s$ ,  $\hat{v}_{\parallel} = v_{\parallel}/v_{thi}$ ,  $\nu_{*i} = \nu_i R q / (\epsilon^{3/2} v_{thi})$  and  $\hat{w} = w/\psi_s$ , together with the dimensionless drift frequencies

$$\omega_{E, x} = \frac{1}{2} \left\langle \frac{\hat{\rho}_{\theta i}}{\hat{v}_{\parallel}} \frac{\partial \hat{\Phi}}{\partial \xi} \right\rangle_{\theta}, \quad \omega_{E, \xi} = \frac{1}{2} \left\langle \frac{\hat{\rho}_{\theta i}}{\hat{v}_{\parallel}} \frac{\partial \hat{\Phi}}{\partial x} \right\rangle_{\theta}, \quad (4)$$

$$\omega_D = \langle \hat{\rho}_{\theta i} \hat{v}_{\parallel} \rangle_{\theta} + L_q \left\langle RB \frac{\partial}{\partial x} \left( \frac{\hat{\rho}_{\theta i} \hat{v}_{\parallel}}{I} \right) \right\rangle_{\theta},$$

with  $\hat{\Phi} = L_q (Ze/T_i) \Phi$ ,  $L_q^{-1} = (1/q) dq/dx$ ,  $\hat{\rho}_{\theta i} = \rho_{\theta i}/\psi_s$  and  $\Theta$  is the Heaviside function.

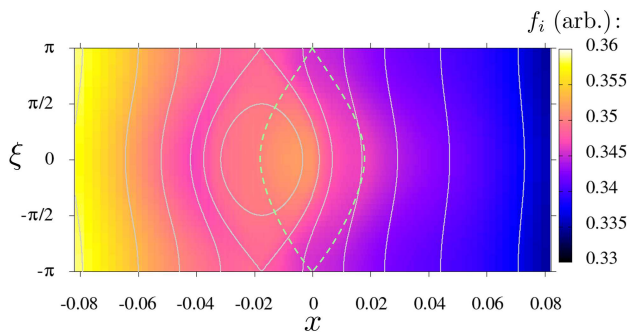


FIG. 1. (Colour online) Colour contour plot of the ion distribution function in the  $x - \xi$  plane obtained from Eq. (3), with the magnetic island separatrix flux surface (dashed) and contours of constant stream function,  $S$  (full).

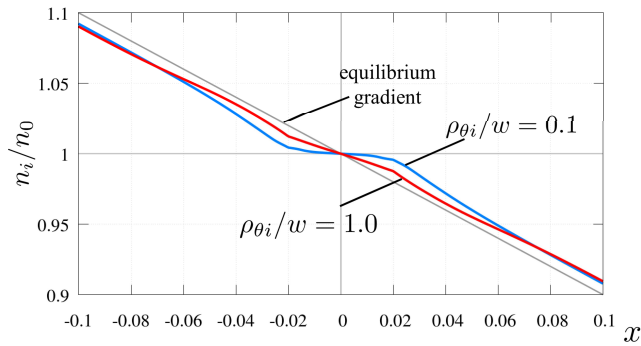


FIG. 2. (Colour online) Radial ion density profile for  $\hat{\rho}_{\theta i}/\hat{w} = 0.1$  and  $\hat{\rho}_{\theta i}/\hat{w} = 1.0$  across the island O-point. Even for small  $\hat{\rho}_{\theta i}$  there is a partial restoration of the flattened density gradient, and the flattening is almost entirely gone for  $\hat{\rho}_{\theta i} \sim \hat{w}$ .

We solve Eq. (3) numerically for arbitrary values of  $\hat{\rho}_{\theta i}$  and  $\hat{w}$ , employing the momentum-conserving model collision operator described in [12]. To determine the normalised electrostatic potential  $\hat{\Phi}$ , we impose the quasi-neutrality condition, which requires a solution for the electron response. Because the electron orbit width is a factor  $(m_e/m_i)^{1/2}$  smaller than that of the ions, we adopt the small  $\rho_{\theta e}/w$  solution described in [5]. To ensure that the collisions correctly account for momentum conservation, we use our numerical solutions for the ion flow in the electron collision operator.

Fig. 1 shows a colour contour plot for the passing particle ion distribution function for parameters:  $\hat{w} = \hat{\rho}_{\theta i} = 0.02$ ,  $L_q/r_s = 1.0$ ,  $\lambda/\lambda_c = 0.1$ ,  $\hat{v} = 1.0$ ,  $\nu_{*i} = 0.01$ ,  $\epsilon = 0.1$ , and  $f(\xi) = \cos \xi$  (likewise for subsequent figures, unless otherwise stated). The island structure is clear in the colour contours, but comparison with the magnetic island flux contours shows a shift in the contours of constant distribution function compared to the magnetic island. To understand this, consider the collisionless limit

of Eq. (3) which, to leading order in  $\Delta$ , can be reduced to the following form:

$$[\hat{p}_\phi \Theta(\lambda_c - \lambda) + \omega_D - \omega_{E,\xi}] \frac{\partial \bar{g}_i^{(0)}}{\partial \xi} \Big|_S = 0, \quad (5)$$

where

$$S = 2 \left[ (\hat{p}_\phi + \omega_D)^2 - \frac{\hat{w}^2}{4} \cos \xi \right] \Theta(\lambda_c - \lambda) + \omega_D \hat{p}_\phi \Theta(\lambda - \lambda_c) - \frac{1}{2} \left\langle \frac{\hat{\rho}_{\theta i}}{\hat{v}_\parallel} \hat{\Phi} \right\rangle_\theta. \quad (6)$$

This function  $S$  is the stream lines for the ions. When the effect of  $\Phi$  is ignored (which represents the effect of the  $\mathbf{E} \times \mathbf{B}$  drift), one can show that the contours of constant  $S$  are identical to the magnetic island flux surfaces, but shifted by a few  $\hat{\rho}_{\theta i}$ . The result of Eq. (5) is that the ion distribution function now only depends on three variables in the low collision frequency limit:  $g_i^{(0)}(x, \theta, \xi, \lambda, v; \sigma) = \bar{g}_i^{(0)}(S, \lambda, v; \sigma)$ . This is the toroidal generalisation of the result from slab geometry (i.e. Eq. (8) of [13]). The dependence on  $S$ ,  $\lambda$  and  $v$  can be derived by introducing collisions at next order to provide another constraint equation [14]. The contours of constant  $S$  are shown as the full curves in Fig 1, confirming that they coincide with the colour contours of the distribution function. We refer to the constant  $S$  island structures as ‘drift islands’.

The shift of the drift island for  $\sigma = +1$  is equal and opposite to that for  $\sigma = -1$ . In constructing the density, one sums over  $\sigma$  before integrating the distribution function over  $\lambda$  and  $v$ . Because the regions where the distribution function is flattened shift in opposite directions for  $\sigma = \pm 1$ , the distribution summed over  $\sigma$  supports substantial gradient inside the magnetic island when  $\hat{w} \sim \hat{\rho}_{\theta i}$ . For large  $\hat{w} \gg \hat{\rho}_{\theta i}$ , the shift in each direction is relatively small, and then the distribution function is approximately flattened across the magnetic island, as expected. However, when  $\hat{w} \sim \hat{\rho}_{\theta i}$  a density gradient is supported inside the island (see Fig. 2). This is a finite orbit width effect — not the well-known transport effect [4]. The strong parallel flows of the electrons tend to flatten their density across the island even for the small island width case. However, the electrons depend on the electrostatic potential also, and their response must adjust to satisfy quasi-neutrality. Our converged solutions do indeed satisfy quasi-neutrality, and the same gradients are supported in the electron density as we see here for the ion density. A similar result was found in [15], which treated only ions and neglected quasi-neutrality effects. Our analysis provides an interpretation, as well as confirming the result in a more accurate plasma model.

To understand the impact of these results on the bootstrap current, we now proceed to consider the ion flows. For the ions the parallel streaming and  $\mathbf{E} \times \mathbf{B}$  flows are

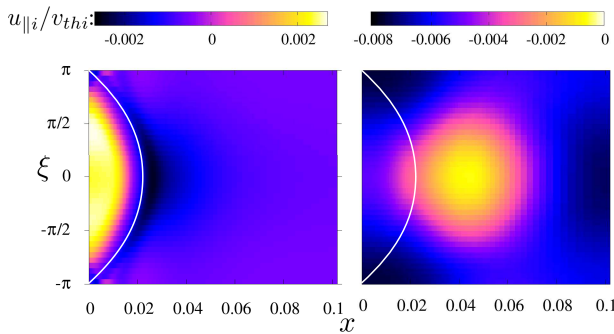


FIG. 3. (Colour online) Contour plots of ion parallel flow,  $u_{||i}$ , on  $x - \xi$  half-plane. The flow profile is approximately symmetric about the island centre ( $x = 0$ ). For small  $\hat{\rho}_{\theta i}/\hat{w} = 0.1$  (left), the flow is largely a flux surface quantity, but for large  $\hat{\rho}_{\theta i}/\hat{w} = 1$  (right), it is entirely different. The white contour shows the position of the magnetic island separatrix.

expected to compete (e.g. see [5, 12]), so it is particularly important that the electrostatic potential is derived consistently with the quasi-neutrality condition. From Fig. 3, it is clear for the small  $\hat{\rho}_{\theta i}$  case that the pattern of the flow around the island follows the perturbed magnetic island geometry and that the flow inside the island separatrix is in the opposite direction to that outside. On the other hand, the case for  $\hat{\rho}_{\theta i} = \hat{w}$  is more complicated — there is a notable variation in the flow within a flux surface, with a broader peak in the profile a few island widths beyond the separatrix.

To calculate the impact on the neoclassical tearing mode drive, we require the current perturbation. Combining our numerically derived ion flows with the analytic theory for the electron neoclassical flows [5], we derive the current averaged over the magnetic island flux surfaces. The contribution to the island evolution is characterised by  $\Delta'_{bs}$ , given by [5]:

$$\psi_s \int_{-\infty}^{\infty} dx \oint J_{bs} \cos \xi d\xi = \frac{c}{32} \frac{r_s}{L_q} \Delta'_{bs} \frac{w^2 B}{Rq}, \quad (7)$$

where  $J_{bs} = \sum_{j=i,e} Z_j e n_j v_{thj} \langle u_{||j} \rangle_{\Omega}$  and  $\langle \dots \rangle_{\Omega} = \oint \dots [\Omega + \cos \xi]^{-1/2} d\xi / \oint [\Omega + \cos \xi]^{-1/2} d\xi$  with  $\Omega = 2x^2/\hat{w}^2 - \cos \xi$  the perturbed flux function describing the island geometry. The flux surface integrals are taken at constant  $\Omega$ .

The results for  $\Delta'_{bs}$  normalised to  $\beta_{\theta}$  as a function of  $\hat{w}$  are shown for a range of  $\hat{\rho}_{\theta i}$  in Fig. 4 ( $\beta_{\theta} = 2\mu_0 p^2/B_{\theta}^2$ , where  $p$  is the plasma pressure). For large  $\hat{w} \gg \hat{\rho}_{\theta i}$  the result asymptotes to the value expected from previous analytic theories [2, 3, 5], which is represented by the dashed line. However, for small island width we see that the impact of the shift of the drift islands compared to the magnetic island is to reduce the bootstrap drive. The negative value of  $\Delta'_{bs}$  at the smallest island widths indicates that the effect of the current perturbation is

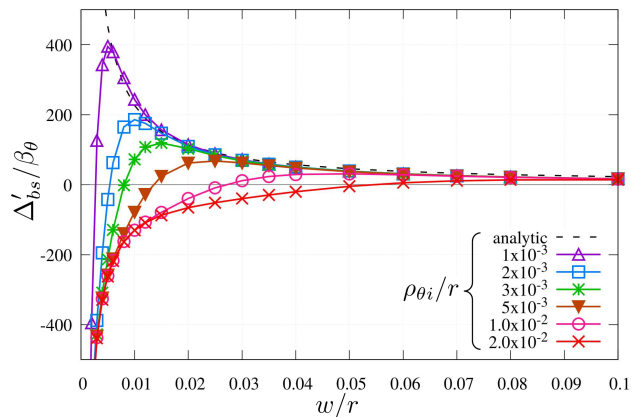


FIG. 4. (Colour online) The bootstrap current contribution to the island evolution,  $\Delta'_{bs}$ , normalised to  $\beta_{\theta}$ , as a function of  $\hat{w}$ , for different values of  $\rho_{\theta i}$ . The black dotted line is the analytic result of [5], for which  $\Delta'_{bs} \propto 1/w$ .

to heal the island — a remarkable and unexpected result. For larger  $\hat{\rho}_{\theta i}$ , the peak value in  $\Delta'_{bs}$  decreases substantially, suppressing the bootstrap drive for the island growth. The critical island width,  $w_c$ , where  $\Delta'_{bs}$  passes through zero, increases linearly with  $\rho_{\theta i}$ : it can be fitted by  $w_c \simeq 2.7\rho_{\theta i}$ .

To understand the physics underpinning the stabilisation of small islands, we plot in Fig. 5 the individual ion and electron current density contributions to  $\Delta'_{bs}$ . Plotting  $\rho_{\theta i} \Delta'_{bs}/\beta_{\theta}$  vs.  $w/\rho_{\theta i}$ , we find that all five  $\rho_{\theta i}/r$  cases condense onto a universal set of curves for the ion and electron contributions. This is a consequence of the parallel flows being proportional to  $\rho_{\theta i,e}$ , as predicted by analytic neoclassical theory. Notice that, as  $w \rightarrow 0$ , the ion contribution to  $\Delta'_{bs}$  tends to zero, consistent with the gradient (and therefore bootstrap current) being unperturbed in this limit. Indeed, we expect that when the island width is much less than the ion banana width, the ions will average over all fields associated with the island. Electrons still respond to the island electromagnetic fields, so an electrostatic potential is established to maintain quasi-neutrality; we postulate that it is the response of the electrons to this potential that creates the stabilising contribution to the current density.

In conclusion, we have presented a new drift kinetic theory for the response of ions to small magnetic islands in tokamak plasmas, and deduced some of the implications for the neoclassical tearing mode threshold physics. Neglecting cross field transport, we find that a consequence of the drifts is that the ion distribution function is not flattened across the magnetic island, but rather across a drift island that is shifted radially compared to the magnetic island. This shift is important for small islands comparable to the trapped ion banana width, in which case a pressure gradient is maintained inside the island. This suppresses the bootstrap current drive for the

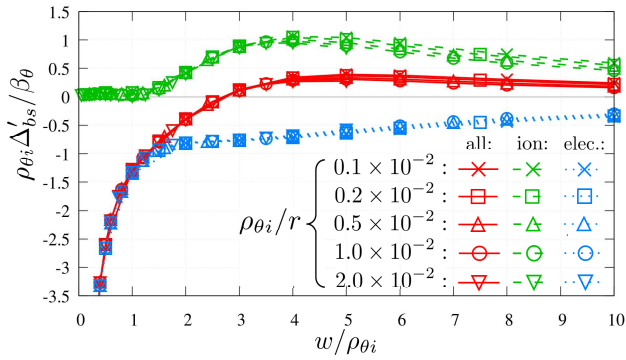


FIG. 5. (Colour online) Plot of  $\rho_{\theta i} \Delta'_{bs} / \beta_{\theta}$ , as a function of  $w / \rho_{\theta i}$ , for different values of  $\rho_{\theta i}$ . Red solid curves represent the total contribution, while green dash and blue dotted curves correspond to ion and electron contributions respectively.

neoclassical tearing mode and the flows are then dominated by the electron physics, tending to heal a sufficiently small seed island. This new physics is important for a complete theory of the neoclassical tearing mode threshold and, in particular, for designing the NTM control system for ITER. Understanding the full implications of our theory for quantifying the NTM threshold will be the subject of future work, including an assessment of the accuracy of our analytic theory for the electron response employed here, the impact of finite ion Larmor radius, and the impact of finite island propagation frequency, including the ion polarisation current physics.

This work was supported by the UK Engineering and Physical Sciences Research Council, grant number EP/N009363/1. Numerical calculations were performed using the ARCHER computing service through the Plasma HEC Consortium EPSRC Grant Number EP/L000237/1, as well as on EUROfusion High Perfor-

mance Computer (Marconi-Fusion).

- 
- [1] R. J. Bickerton, J. W. Connor, and J. B. Taylor, *Nature Physical Science* **229**, 110 (1971).
  - [2] See National Technical Information Service Document No. DE608946 (W.X. Qu and J.D. Callen, University of Wisconsin Plasma Report No. UWPR 85-5, 1985). Copies may be ordered from the National Technical Information Service, Springfield, VA 22161.
  - [3] R. Carrera, R. D. Hazeltine, and M. Kotschenreuther, *Physics of Fluids* **29**, 899 (1986).
  - [4] R. Fitzpatrick, *Physics of Plasmas* **2**, 825 (1995).
  - [5] H. R. Wilson, J. W. Connor, R. J. Hastie, and C. C. Hegna, *Physics of Plasmas* **3**, 248 (1996).
  - [6] A. B. Mikhailovskii, V. D. Pustovitov, and A. I. Smolyakov, *Plasma Physics and Controlled Fusion* **42**, 309 (2000).
  - [7] A. Bergmann, E. Poli, and A. G. Peeters, *Physics of Plasmas* **12**, 072501 (2005).
  - [8] E. Poli, A. Bergmann, and A. G. Peeters, *Physical Review Letters* **94**, 205001 (2005).
  - [9] W. A. Hornsby, M. Siccino, A. G. Peeters, E. Poli, A. P. Snodin, F. J. Casson, Y. Camenen, and G. Szepesi, *Plasma Physics and Controlled Fusion* **53**, 054008 (2011).
  - [10] R. J. L. Haye, R. Prater, R. J. Buttery, N. Hayashi, A. Isayama, M. E. Maraschek, L. Urso, and H. Zohm, *Nuclear Fusion* **46**, 451 (2006).
  - [11] W. A. Hornsby, P. Migliano, R. Buchholz, S. Grosshauser, A. Weigl, D. Zarzoso, F. J. Casson, E. Poli, and A. G. Peeters, *Plasma Physics and Controlled Fusion* **58**, 014028 (2016).
  - [12] K. Imada and H. R. Wilson, *Plasma Physics and Controlled Fusion* **51**, 105010 (2009).
  - [13] F. L. Waelbroeck, J. W. Connor, and H. R. Wilson, *Physical Review Letters* **87**, 215003 (2001).
  - [14] A. Dudkovskaia, J. W. Connor, P. Hill, K. Imada, and H. R. Wilson, In preparation.
  - [15] E. Poli, A. G. Peeters, A. Bergmann, S. Günter, and S. D. Pinches, *Physical Review Letters* **88**, 075001 (2002).